Results in Engineering 24 (2024) 103613

Contents lists available at ScienceDirect

Results in Engineering

journal homepage: www.sciencedirect.com/journal/results-in-engineering

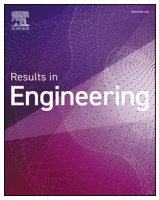

Research paper

Using structural equation modeling and intima-media complex texture features to assess cardiovascular disease risk in the common carotid artery

George Evripides [a], Christos P. Loizou [a], Paul Christodoulides [b,*]

[a] Department of Electrical Engineering, Computer Engineering and Informatics, Cyprus University of Technology, Limassol, Cyprus
[b] Faculty of Engineering and Technology, Cyprus University of Technology, Limassol, Cyprus

ARTICLE INFO

Keywords:
Cardiovascular disease (CVD)
Texture analysis
Common carotid artery (CCA)
Structural equation modeling
Moderating effect of Intima-media thickness (IMT)

ABSTRACT

The potential for stroke risk in humans due to clinical cardiovascular disease (CVD), which leads to the hardening of the artery walls (atherosclerosis), can be assessed by examining the common carotid artery (CCA) in ultrasound images. Specifically, this can be done by measuring the intima media thickness (IMT), which represents the thickness of the arteries wall, and by analyzing texture features (TFs) of the CCA's intima-media complex (IMC) of the artery wall. In this paper, a sample of 612 longitudinal-section ultrasound images of the left and the right CCA from 158 men and 148 women, out of which 42 demonstrated clinical CVD, is studied. All images are intensity normalized and despeckled, with the IMC segmented through an in-house system of semi-automated segmentation, where the IMT is measured, and 40 different TFs are extracted. Then, employing structural equation modeling (SEM), these TFs, which are put in 6 groups (constructs), are collectively tested on how they are related to CVD. The influence of the IMT is also studied through a moderation analysis, while gender and age of the sub-jects of the study are tested with regard to their control effect. The main conclusions of the study are as follows. The 6 TFs groups and the IMT fit the measurement model very well. Also, 6 hypothesized paths for the impact of each TFs group on CVD are tested in a structural model, with 5 of them, namely Statistical Features (SF), Spatial Gray Level Dependence Matrices (SGLDM), Gray Level Difference Statistics (GLDS), Statistical Feature Matrix (SFM) and Laws Texture Energy Measures (LTEM), impacting CVD in a moderate manner (p-values between 0.04 and 0.07). The IMT is shown to play a strong moderating role (p-values of $\Delta\chi^2 < 0.01$), enhancing the level of impact of the TFs on CVD. Gender and age have a strong controlling effect on CVD (p-values of < 0.01). The precision of the findings of this study is considerably improved compared to those previously reported, because of the very good model fit (e.g., normed fit index (NFI) = 0.94) for both measurement and structural models. However, due to the moderate nature of the impact, supplementary work is required for testing either additional combinations of TFs, as well as testing other samples through the proposed model, for further evaluation of the CVD risk on symptomatic subjects at risk of atherosclerosis.

1. Introduction

Cardiovascular disease (CVD) ranks first in mortality and morbidity [1]. Although ischemia or arrhythmias are important contributors [2], atherosclerosis is the main cause of CVD, which includes myocardial infarction, heart failure, and stroke [3–7]. Non-invasive ultrasound imaging techniques are frequently used to monitor the process of atherosclerosis [4], by recognizing common carotid artery (CCA) stenosis and measuring the arterial wall thickness – known as the intima-media thickness (IMT). The IMT can be seen and quantified by identifying the double line pattern along both the far and near walls of the longitudinal images of the CCA (see also Fig. 1). It has been demonstrated that an increased IMT of the CCA is related with an increased risk of myocardial infarction and stroke, particularly in older persons without any history of CVD [3]. The IMT of the human CCA can be estimated by a noninvasive technique, namely B-mode ultrasound [3,7]. As a result, the IMT can be used to screen populations, potentially averting at least half of all early heart attacks and strokes [3–5,8]. The IMT has conventionally been utilized as a CVD biomarker, but it has been found and verified unsuccessful in the prediction of future CVD events based on conventional risk indicators [3–7] (see also Fig. 1). Instead, texture features (TFs) extracted from the intima-media complex

* Correspondence author.
E-mail address: paul.christodoulides@cut.ac.cy (P. Christodoulides).

https://doi.org/10.1016/j.rineng.2024.103613
Received 13 August 2024; Received in revised form 28 November 2024; Accepted 2 December 2024
Available online 2 December 2024

(IMC) of the CCA wall in ultrasound images, as well as other characteristics, may provide additional and more precise information about the course of atherosclerosis. Hence, they may be utilized, together with the IMT, for giving information for the assessment of CVD risk, and predicting imminent CVD events [4–6,9]. In Fig. 1 ultrasound images of the left (L) and right (R) CCA side, show the semi-automated segmentation of the IMC at the far wall of the artery, which was performed using an integrated software system [4,5]. The IMC represents the layer of the artery mostly affected by atherosclerosis, where the L side and R sides are different and may also contribute differently to the risk of stroke [4,7]. Given the distinct anatomy of each CCA side (L vs. R), it has been postulated – although not completely researched – in the literature, that the various risk factors have different impacts on the L vs. R CCA side [10]. The reason for the observed differences between the L and R sides CCA sides is currently unknown. It is hypothesized that these disparities could be attributed to the fact that the distinct origins of the L and R CCA sides lead to varying flow intensities from the aortic arch. The L CCA originates directly from the aortic arch, influenced by its pressure. On the other hand, the R CCA stems from an extension of the ascending aorta, namely the innominate artery, experiencing significant pressure from the ascending aortic blood flow. Additionally, in previous studies the interaction between blood and the intima causing wall shear stress has been linked to the development of atherosclerotic plaque and, hence, thick IMT as well as vascular structural remodeling [10]. Studies in the literature [11] have suggested that the progression of the IMT speeds up in older individuals, potentially explaining the variation in IMT between older and younger patients [5]. It is hypothesized that if mechanical shear stress plays a role in accelerating the development of atherosclerosis in the L CCA, it may take a considerable amount of time for this effect to become apparent [10].

The impact of TFs of the IMC on IMT and CVD has been the subject of recent studies through the use of structural equation modeling (SEM) [6,9]. SEM is a collection of techniques that are commonly used to evaluate theoretical models that incorporate suggested causal links between a set of variables [12]. In this way, SEM can be thought of as a confirmatory approach for assessing structural relationships between variables. Nevertheless, SEM is flexible enough to accommodate exploratory data analysis. For example, in social sciences using SEM is typically justified by its ability to identify relationships between unobserved constructs (latent factors) and observable variables [13–15]. In general, SEM could be used to represent, estimate, and evaluate a network of relationships between variables. SEM includes measurement, correlational analysis, path analysis, regression modeling, and equations, and it assumes that planned relationships among variables can be represented in by structural regression equations, with successive relationships portrayed pictorially, to test hypotheses about the relationships between variables, thereby testing a theoretical network of (mainly) linear relationships between variables [16,17].

As SEM may be suited to researching situations that find systems of relationships rather than fitting regression models of one dependent variable and a number of predictors or independent variables, it has been suggested that SEM could be a useful tool in modeling complex biological pathways [18,19]. In particular, an investigation of the associations between CVD risk factors, carotid atherosclerosis, and cognitive function within a Canadian First Nations population, performed using SEM, revealed that individuals with elevated levels of left and total CCA stenosis (LCS and TCS) had lower chance of demonstrating lowered performance [18]. It was found that people with high levels of LCS and TCS had lower chance of having poor cognitive function and that anthropometric risk factors were connected with a decreased percentage of TCS but an increased risk of poor cognitive performance. Given a reasonable biological explanation, the findings support the relevance of vascular variables and disease in executive-derived cognitive function. [18]. In another study, SEM was performed to test the hypothesis that obesity affects the IMT, resulting in evidence for an indirect effect through other CVD risk factors [19]. The authors concluded that traditional CVD risk factors had important direct effects on IMT in adolescents and young adults, but adiposity could exercise its influence indirectly through other CVD risk factors.

By employing SEM, the current study intends to collectively examine how the IMC TFs are related to CVD, with consideration given to the influence of the IMT as well. The ultimate goal would be the exploration of how SEM analysis of ultrasound imaging IMC quantities (TFs and IMT) might be used to predict the CVD risk. Specifically, SEM will evaluate the relationships between the IMC TFs and the prevalent clinical CVD using the IMT quantity as a moderator. It should be mentioned that the IMC is semi-automatically segmented through an integrated snake segmentation technique based on active contours [5,7]. It should also be mentioned that both the L and R CCA sides are used as distinct parameters (items). To the best of our knowledge no similar studies exist in the literature with regard to the relationships considered here for determining factors to assess CVD risk, using the multifold analysis provided by SEM.

The methodology presented in the current investigation has recently been used, but the SEM fits did not produce satisfying results, implying that the findings' dependability could have been problematic [6]. More specifically, in that study IMT was treated as an observable variable rather than a latent variable. Furthermore, the results reported were not sufficiently reliable due to a poor fit between the data and the proposed structural model. It was further suggested that those results could be improved by considering additional metrics such as: (i) sample size expansion, (ii) model size increase, (iii) additional hypotheses among

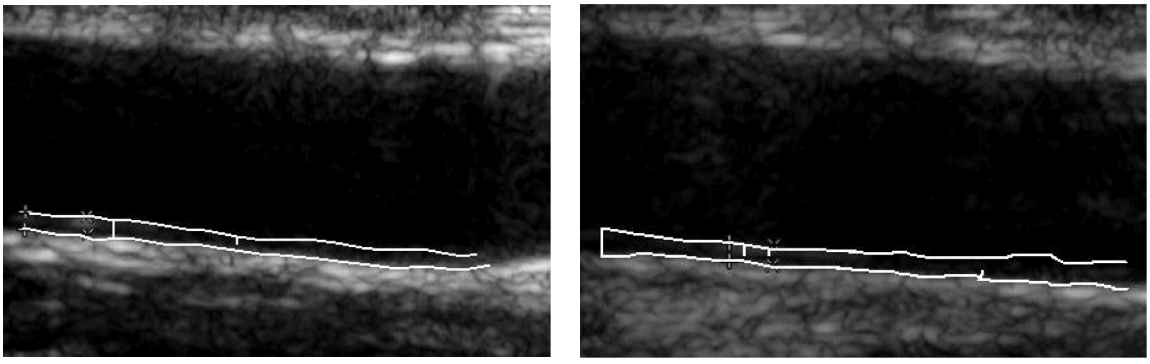

Fig. 1. Ultrasound images of the CCA with the semi-automated segmentation of the IMC at the far wall, which represents the layer of the artery mostly affected by atherosclerosis: Mean, median, minimum and maximum values of the IMT for the L side CCA (a) $IMT_{mean} = 0.72$ mm, $IMT_{median} = 0.78$ mm, $IMT_{max} = 0.89$ mm, $IMT_{min} = 0.56$ mm and (b) the right (R) side of the CCA with $IMT_{mean} = 0.97$ mm, $IMT_{median} = 0.93$ mm, $IMT_{max} = 1.24$ mm and $IMT_{min} = 0.73$ mm respectively.

latent variables, (iv) variables merge, and (v) higher Likert style scale. In a subsequent study [9], some of the above-mentioned measures were adopted, and the TFs, together with the IMT, were used as latent variables, while CVD was introduced as an observable variable. The equations with software (EQS), a SEM software that provides a simple approach for doing the full range of SEM studies and extremely accurate statistics for multivariate, not necessarily normally distributed, data, is utilized here [12].

2. Materials and methods

2.1. Acquisition of images segmentation and texture features extraction

A Philips ATL HDI-5000 ultrasound duplex scanner (Seattle, WA, USA) recorded 612 B-mode longitudinal ultrasound images of the L and R CCA sides, displaying the vascular wall as a regular pattern associated with anatomical layers (see also Fig. 1), for 306 individuals (158 men and 148 women), from two mountain villages in Cyprus. Out of these, 42 had clinical CVD [4,7]. Images were captured with a resolution of 576 × 768 pixels and 256 gray levels. All images were re-sized using bicubic spline interpolation to a standard pixel density of 16.66 pixels/mm (resulting in a pixel width of 0.06 mm). The intensity of each of the 612 (306 L and 306 R) ultrasound images was normalized, by performing brightness adjustments, with ultrasound tissue comparability facilitated, using a widely used methodology [4–6,7,20]. More specifically, as proposed in previous studies from the authors group, algebraic (linear) scaling, image intensity normalization, image resizing to standard pixel density, brightness readjustment and despeckle filtering were all performed on the images, prior to the IMT measuring and IMC texture features (TFs) extraction [3–5,7,20]. This enhancement increases image compatibility by minimizing the discrepancies caused by various gain settings, operators, equipment, and allows for easier ultrasound tissue comparison. Finally, the images underwent both manual and automated segmentation of the IMC, with the CCA's IMT being measured. Manual segmentations were performed by an expert neurologist (who provided the measurements IMT1, IMT2 for L and R CCA sides, see Section 3, Table 2) [5–7], while automated segmentations were performed by an IMC integrated segmentation system [5] (providing the IMT3, IMT4 measurements for L and R CCA sides, see Section 3, Table 2), for the L and R CCA sides respectively [5,7]. It must be though noted that for the TFs extraction, only the automated segmentations were used, as these provide complementary information for the risk of stroke [4,5,7].

A total of 26 different TFs were used as construct items (for 6 latent variables) from the provided imaging sample. In addition, construct IMT (with its four measured items) along with Gender and Age were also used as moderator and controls (see, for example, [21]) on the observable variable CVD, as shown in Fig. 2. The TFs were extracted from the automated segmented IMC image regions of interest and are described below [15,20,22,23]:

(i) Statistical Features (SF): TFs (items) SF 1–4, namely mean intensity (SF1) and median intensity (SF2), standard deviation and kurtosis [22].
(ii) Spatial Gray Level Dependence Matrices (SGLDM): TFs SGLDM 1–6, namely, sum average (SGLDM1), entropy (SGLDM2), contrast (SGLDM3), correlation (SGLDM4), and information measures of correlation (IMOC1, IMOC2) i.e., SGLDM5 and SGLDM6 [7,22–24].
(iii) Gray Level Difference Statistics (GLDS): TFs GLDS 1–8, namely sum average GLDS1), correlation (GLDS2), entropy (GLDS3), information measures of correlation (GLDS4, GLDS5), contrast (GLDS6), angular second moment (GLDS7) and sum entropy (GLDS8) [23].
(iv) Statistical Feature Matrix (SFM): TFs SFM 1–4, namely coarseness (SFM1), contrast (SFM2), periodicity (SFM3), and roughness (SFM4) [23,25].
(v) Laws Texture Energy Measures (LTEM): TFs LTEM 1–2, namely EE- texture energy from EE-kernel (LTEM1) and LL-texture energy from LL kernel (LTEM2) [26].
(vi) Fractal Dimension Texture Analysis (FDTA): TFs FDTA 1–4, namely the Hurst coefficients for dimensions 1–4 were computed (HC1, HC2, HC3, HC4) [22,26].

All the above features were saved for further analysis and evaluation.

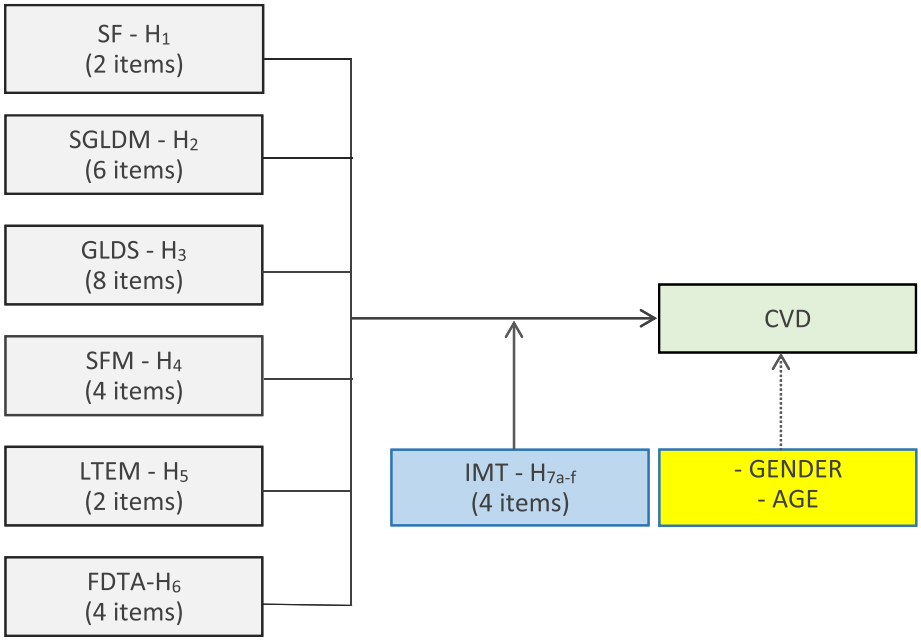

Fig. 2. The proposed conceptual model used in this study; hypotheses H1–H6, moderated by the IMT (hypotheses H7a-f). Gender and age are control variables. IMT and TFs extracted from the IMC of the L and R CCA images: SF: Statistical features, SGLDM: Spatial gray level dependence matrix, GLDS: Gray level difference statistics, SFM: Statistical features matrix, LTEM: Laws texture energy measures, FDTA: Fractal dimension texture analysis.

2.2. Model, research instrument and hypotheses

Following the analysis described above, the proposed conceptual model consists of 8 different variables categorized into three different groups, as shown in Fig. 2. The 6 TFs categories (groups), namely SF, SGLDM, GLDS, SFM, LTEM and FDTA, are hypothesized to impact the progression of CVD and thus CVD may be assessed using the above features, as also indicated in a previous preliminary study [9]. The link between the 6 different TFs and CVD is hypothesized to be also moderated by the IMT. In addition, age and gender are used as control variables.

For the purposes of SEM, all the above presented variables, with the exception of CVD, were transformed into a seven-point Likert scale [9], as follows:

$$1: \text{ corresponds to value } \nu \leq \mu - 3\sigma,\ 2: \mu - 3\sigma < \nu \leq \mu - 2\sigma,\ 3: \mu - 2\sigma < \nu \leq \mu - \sigma,$$

$$4: \mu - \sigma < \nu \leq \mu + \sigma,\ 5: \mu + \sigma < \nu \leq \mu + 2\sigma,\ 6: \mu + 2\sigma \langle \nu \leq \mu + 3\sigma,\ 7: \nu \rangle \mu + 3\sigma,$$

where μ is the mean and σ the standard deviation (S.D.) of the sample population of TFs for each TF investigated for the L and R sides IMC of the CCA. The value of CVD is 1 for individuals diagnosed with clinical cardiovascular disease, and 0 for asymptomatic ones (those with no CVD symptoms detected).

Note that, as previously predicted [6], using a 7-point Likert scale instead of a 5-point Likert scale, along with an elliptical re-weighted least-squares approach, increased the accuracy of both the measurement and structural models, as shown in Table 1. In Table 1 one can observe the comparative results for previous SEM cases studied, where on one occasion the same 6 TFs groups were used as latent variables, with IMT being the observable variable [6], and on another occasion the 6 TFs groups along with IMT were the latent variables, with CVD being the observable variable [9]. Regarding the fit indices, a Normed Fit Index (NFI) or a Non-Normed Fit Index (NNFI) (preferable for small samples) of 1 shows a perfect fit of the model. The Comparative Fit Index (CFI) is a revised form of NFI, which is not very sensitive to sample size. The Root Mean Square Error of Approximation (RMSEA) is a

Table 1
Comparison between 5-point and 7-point Likert scales.

Measurement model for case studied in [6]			
Fit Indices	Likert Scale: 5 Elliptical re-weighted least square approach	Likert Scale: 7 Non-elliptical re-weighted least square approach	Likert Scale: 7 Elliptical re-weighted least square approach
Chi-square (χ^2) / Degrees of Freedom (df) ratio ($p = .000$)	1982.54 / 443 = 4.48	4401.26 / 384 = 11.46	1381.78 / 384 = 3.60
Normed Fit Index (NFI)	0.81	0.84	0.94
Non-Normed Fit Index (NNFI)	0.80	0.84	0.95
Comparative Fit Index (CFI)	0.82	0.86	0.96
Root Mean Square Error of Approximation (RMSEA)	0.106	0.097	0.049
Structural Model for case studied in [6]			
Fit Indices	Likert Scale: 5 Elliptical re-weighted least square approach	Likert Scale: 7 Non-elliptical re-weighted least square approach	Likert Scale: 7 Elliptical re-weighted least square approach
Chi-square (χ^2) / Degrees of Freedom (df) ratio ($p = .000$)	2225.89 / 458 = 4.86	5067.39 / 399 = 12.70	1500.51/ 399 = 3.76
Normed Fit Index (NFI)	0.74	0.75	0.89
Non-Normed Fit Index (NNFI)	0.73	0.74	0.90
Comparative Fit Index (CFI)	0.75	0.74	0.91
Root Mean Square Error of Approximation (RMSEA)	0.114	0.128	0.069
Measurement Model for case studied in [9]			
Fit Indices	Likert Scale: 5 Elliptical re-weighted least square approach	Likert Scale: 7 Non-elliptical re-weighted least square approach	Likert Scale: 7 Elliptical re-weighted least square approach
Chi-square (χ^2) / Degrees of Freedom (df) ratio ($p = .000$)	2576.73 / 449 = 5.74	4524.79 / 406 = 11.14	1460.37 / 406 = 3.60
Normed Fit Index (NFI)	0.71	0.84	0.94
Non-Normed Fit Index (NNFI)	0.75	0.83	0.94
Comparative Fit Index (CFI)	0.79	0.85	0.94
Root Mean Square Error of Approximation (RMSEA)	0.114	0.096	0.049
Structural Model for case studied in [9]			
Fit Indices	Likert Scale: 5 Elliptical re-weighted least square approach	Likert Scale: 7 Non-elliptical re-weighted least square approach	Likert Scale: 7 Elliptical re-weighted least square approach
Chi-square (χ^2) / Degrees of Freedom (df) ratio ($p = .000$)	2654.95 / 470 = 5.65	4988.23 / 427 = 11.68	1715.33 / 427 = 4.02
Normed Fit Index (NFI)	0.72	0.72	0.89
Non-Normed Fit Index (NNFI)	0.76	0.70	0.90
Comparative Fit Index (CFI)	0.77	0.73	0.90
Root Mean Square Error of Approximation (RMSEA)	0.095	0.150	0.077

parsimony-adjusted index, with 0 representing the perfect fit. Chi-square assesses the overall fit and the discrepancy between the sample and fitted covariance matrices and is sensitive to sample size. Note that, the indices for good fit are respectively $\chi^2/df \leq 3$ (good) or ≤ 2 (very good), NFI, NNFI, CFI ≥ 0.90 (good) or ≥ 0.95 (very good), RMSEA ≤ 0.08 (good) or ≤ 0.06 (very good) [27]. Hence, the results shown in Table 1 confirm the superiority of using an elliptical re-weighted least square approach, but more importantly that a 7-point Likert scale is more appropriate than a 5-point Likert scale in this application.

The pre-specified correlations between constructs and their indicators were then examined to guarantee construct reliability and validity (see also Table 2). Only elements with high enough standardized loadings (β) were retained for each TF. The structural model was then examined to test the conceptual model's hypothesized paths [28] (refer to Table 4).

There are 6 major theorized pathways presented in this study (see Fig. 2), which are based on the results of [9], as given below:

H_1: The higher the value of the SF TFs, the lower the possibility of CVD.
H_2: The higher the value of the SGLDM TFs, the higher the possibility of CVD.
H_3: The higher the value of the GLDS TFs, the lower the possibility of CVD.
H_4: The higher the value of the SFM TFs, the higher the possibility of CVD.
H_5: The higher the value of the LTEM TFs, the higher the possibility of CVD.
H_6: The higher the value of the FDTA TFs, the higher the possibility of CVD.

Table 2
Measurement model - summary of construct measurements.

Construct/ Scale items	Item β	Item t	Construct α / ρ / AVE	Construct Mean / S.D.	Item mean	Item S.D.
SF1	.58	*	0.51	4.16	4.20	0.69
SF2	.60	8.00	0.44	0.54	4.12	0.63
			0.35			
SGLDM1	.64	*	0.89	4.96	4.09	0.63
SGLDM2	.78	11.81	0.71	0.41	4.02	0.18
SGLDM3	.99	14.19	0.65		4.06	0.43
SGLDM4	.99	14.14			4.06	0.44
SGLDM5	.74	11.37			4.05	0.56
SGLDM6	.62	9.77			4.05	0.66
GLDS1	.68	*	0.89	4.03	4.05	0.68
GLDS2	.70	10.81	0.78	0.50	4.04	0.70
GLDS3	.73	11.18	0.50		4.05	0.62
GLDS4	.76	11.58			4.05	0.61
GLDS5	.70	10.86			3.96	0.67
GLSS6	.71	10.94			3.96	0.68
GLDS7	.69	10.64			4.05	0.65
GLDS8	.69	10.66			4.04	0.68
SFM1	.91	*	0.97	3.96	3.95	0.39
SFM2	.91	26.85	0.86	0.36	3.96	0.38
SFM3	.98	35.13	0.89		3.96	0.37
SFM4	.97	32.93			3.97	0.35
LTEM1	.61	*	0.54	3.92	3.92	0.65
LTEM2	.61	14.69	0.47	0.55	3.93	0.67
			0.37			
FDTA1	.70	*	0.78	3.91	3.97	0.66
FDTA2	.73	11.79	0.55	0.52	3.96	0.64
FDTA3	.64	10.35	0.47		3.85	0.68
FDTA4	.66	10.74			3.88	0.68
IMT1	.67	*	0.79	3.93	3.95	0.74
IMT2	.65	9.72	0.75	0.56	3.89	0.74
IMT3	.75	10.97	0.51		3.94	0.68
IMT4	.72	10.64			3.93	0.68

* Item fixed to set the scale (β = standardized loadings)
Fit statistics of Model: $\chi^2 = 1460.37$, $p = .000$, df = 406, NFI = 0.94, NNFI = 0.95, CFI = 0.95, RMSEA = 0.049.

In SEM moderation refers to the interaction effect between two variables on a third variable [27,28]. Moderation occurs when the relationship between two variables varies, depending on the level of a third variable. In other words, the strength and direction of the relationship between two variables are not constant across different levels of the third variable. It is also known as interaction or conditional effect. Here, given the character of the IMT, we can posit the following hypotheses pointing to the moderating role of IMT in this framework:

H_{7a}: The link between SF and CVD becomes stronger when IMT is high.
H_{7b}: The link between SGLDM and CVD becomes stronger when IMT is high.
H_{7c}: The link between GLDS and CVD becomes stronger when IMT is high.
H_{7d}: The link between SFM and CVD becomes stronger when IMT is high.
H_{7e}: The link between LTEM and CVD becomes stronger when IMT is high.
H_{7f}: The link between FDTA and CVD becomes stronger when IMT is high.

3. Results

3.1. Measurement model

The measurement model was validated through a confirmatory factor analysis on the model's constructs, which limits each item to loading on its predetermined factor, and simultaneously allows the underlying factors to correlate [19]. The estimation of the measurement model was done through an elliptical reweighted least-squares approach in EQS, which indicated a very good fit to the data ($\chi^2 = 1460.37$, $p = 0.000$, degrees of freedom (df) = 406, NFI = 0.94, NNFI = 0.95, CFI = 0.95, RMSEA = 0.049; refer to Table 2) (see also [6,9,27]).

Regarding the statistics of Table 2, a factor loading (β) is basically the correlation coefficient for the variable (item) and factor (construct). Factor loading demonstrates the variance explained by the variable on that particular factor. As a rule of thumb, $\beta \geq \sim 0.6$ represents a factor that extracts sufficient variance from that variable. The t-value measures the size of the difference relative to the variation in the sample data; the greater the magnitude of t, the better the fit (significance), with $t \geq 2.575$ representing a probability value $p \leq 0.01$ for error. Note that, out of a total of 40 IMC TFs extracted for the purposes of this study, the ones selected for the analysis here were the ones with large enough factor loading values (see also [6,9]).

The collected data underwent a purification process through the following four phases:

(i) All the variables were checked for convergent validity, which was met as the t-value of each variable was always high and statistically significant and all standard errors of the estimated coefficients were very low, although not all average variances extracted (AVE) for each construct were ≥ 0.50 [28]. Convergent validity denotes the degree to which two measures of constructs that should theoretically be related, are actually related.
(ii) The discriminant validity was assessed and found to be satisfied, as the confidence interval around the correlation – calculated for each pair of items – never contained 1 [19], while the squared correlation for each pair of constructs never exceeded their AVE [29] (see Table 3). Discriminant validity determines whether measurements or concepts that are supposed to be unrelated are actually unrelated.
(iii) The construct reliability was examined and found to be acceptable, as all but two constructs in our conceptual model had Cronbach's $\alpha > 0.60$; likewise, the composite reliability was found to be acceptable, as all but two coefficients $\rho > 0.55$ [30].

Table 3
Correlation matrix of the model factors for all TFs groups investigated in this study.

	Constructs	1	2	3	4	5	6	7	8
1	SF	*.59*							
2	SGLDM	−0.46	*.81*						
3	GLDS	.39	−0.46	*.71*					
4	SFM	.33	−0.48	.48	*.94*				
5	LTEM	−0.49	.47	−0.27	−0.36	*.61*			
6	FDTA	.47	−0.48	.46	.45	−0.44	*.69*		
7	IMT	.40	.49	.47	.41	−0.41	.47	*.71*	
8	CVD	−0.19	.05	−0.01	.09	.07	.47	.48	*N/A*

Note: Correlations > |± 0.08| are significant at the 0.01 level; correlations > |±0.05| are significant at the 0.05 level; values below the diagonal refer to correlation estimates among constructs, and values on the diagonal refer to square root of AVE.

Construct reliability refers to how consistent the measuring of a specific construct is, indicating internal consistency and reliability. Composite reliability refers to how consistent multiple measurements of a construct are.

(iv) Finally, the potential of a common method bias was investigated. Common method bias arises when the same method (or tool) is used to collect data from different sources, resulting in an over-representation of specific factors. In particular, the Harman's single-factor test was used [30] in a principal component analysis with varimax rotation that involved all items. The unrotated factor solution resulted in 8 distinct factors with eigenvalues > 1.0, which explained 67.9 % of the total variance (with the first factor explaining 11.5 %). Additionally, a confirmatory factor procedure was implemented, where all items of the measurement model were restricted to loading on a single factor [31]. The model fit indices were considerably below frequently accepted cut-off points ($\chi^2 = 6870.52$, $p = 0.000$, df = 366; NFI = 0.65, NNFI = 0.64, CFI = 0.67, RMSEA = 0.12). Hence, the findings of both tests demonstrate that common method bias is not present in this study.

3.2. Structural model

3.2.1. Direct effects

Table 4 shows the results of the proposed structural model. The estimation of the structural model was done through an elliptical re-weighted least-squares approach in EQS, which revealed a very good fit to the data ($\chi^2 = 1190.09$, $p = .000$, df = 355, NFI = 0.93, NNFI = 0.94, CFI = 0.95, RMSEA = 0.046). All, but one, hypotheses are accepted. Constructs (TFs groups) SGLDM, SFM and LTEM have a positive effect on CVD (see positive t-values and $p < .10$ for hypotheses H_2, H_4, H_5), i.e., high SGLDM, SFM and LTEM values yield high possibility of CVD. In particular, SGLDM and SFM had a higher effect on CVD with $p < .05$. It also turns out that SF and GLDS have a negative effect on CVD (see negative t-values and $p < .10$ for hypotheses H_1 and H_3), i.e., high SF and GLDS values yield low possibility of CVD. On the other hand, H_6 is rejected ($p > .10$), meaning that FDTA has no effect on CVD.

Table 4
Structural model - summary of the results.

Hypothesized association	Standardized path coefficient	t-value	p-value	Status
H_1 SF → CVD	−0.23	−1.94	.05	Accepted
H_2 SGLDM → CVD	.15	2.10	.04	Accepted
H_3 GLDS → CVD	−0.13	−1.80	.07	Accepted
H_4 SFM → CVD	.16	2.01	.04	Accepted
H_5 LTEM → CVD	.18	1.79	.07	Accepted
H_6 FDTA → CVD	.09	1.05	.29	Rejected
Control effects				
Gender → CVD	.20	2.28	.02	Accepted
Age → CVD	.74	3.78	.00	Accepted

Fit statistics of Model: $\chi^2 = 1190.09$, $p = .000$, df = 355, NFI = 0.93, NNFI = 0.94, CFI = 0.95, RMSEA = 0.046.

In addition, the control role of gender and age on CVD were tested. It turned out that both controls had a statistically significant effect (gender: $\beta = 0.20$, $t = 2.28$, $p = .02$; age: $\beta = 0.74$, $t = 3.78$, $p = .00$), as predicted by the statistics of the sample. Male subjects were represented by a '1′ value, while female subjects by '2′. Females seem to be of higher CVD risk than males. Likewise, age (separated into three groups, namely '1′ for subjects younger than 50 years old, '2′ for subjects of age between 50 and 70, and '3′ for subjects older than 70 years old) seems to play a statistically significant effect ($\beta = 0.74$, $t = 3.78$, $p = .00$), showing that age enhances CVD.

3.2.2. Moderation effects

The split group method (based on the median) was used to identify subsamples of values for the IMT as moderator (either low or high; see Table 5). The moderator was found to have a statistically significant effect ($\Delta\chi^2 = 8.86$, $p < .01$) in the case of the first link, SF → CVD (H_{7a}). Specifically, the impact of SF on CVD was confirmed to be negative for high IMT ($\beta = -0.90$, $t = -2.76$, $p < .01$), as opposed to positive for low IMT ($\beta = 0.21$, $t = 82.86$, $p < .01$). This finding is in line with the fact, accepted in the literature [3,4,5,6,7], that the higher the thickness of the IMC is, the higher the possibility of a CVD is. An exactly similar result ($\Delta\chi^2 = 9.68$, $p < .01$) follows for the third link, GLDS → CVD (H_{7c}), where the impact of GLDS on CVD was confirmed to be negative for high IMT ($\beta = -0.15$, $t = -1.97$, $p < .05$), as opposed to positive for low IMT ($\beta = 0.15$, $t = 2.19$, $p < .05$).

On the other hand, the moderator was found to have a statistically significant effect ($\Delta\chi^2 = 9.02$, $p < .01$) in the case of the second link, SGLDM → CVD (H_{7b}), but the impact of GLDS on CVD was confirmed to be positive and more significant for high IMT ($\beta = 0.91$, $t = 11.91$, $p < .01$), as opposed to low IMT ($\beta = 0.13$, $t = 0.53$, $p > .10$). Exactly similar results are obtained for the fourth and fifth links, SFM → CVD (H_{7d}) ($\Delta\chi^2 = 9.09$, $p < .01$), LTEM → CVD (H_{7e}) ($\Delta\chi^2 = 8.60$, $p < .01$), where the impact of SFM on CVD was confirmed to be positive and more significant for high IMT ($\beta = 0.25$, $t = 3.59$, $p < .01$), as opposed to low IMT ($\beta = 0.14$, $t = 1.23$, $p > .10$), and the impact of LTEM on CVD was confirmed to be positive and more significant for high IMT ($\beta = 0.23$, $t = 2.95$, $p <$

Table 5
Results of IMT as a moderator.

Main effect	Hypothesized moderating effect	Low IMT group	High IMT group	$\Delta\chi^2$ (Δdf = 1)
SF → CVD	H_{7a}: Effect is stronger when IMT is higher	$\beta = 0.21$ $t = 2.86$	$\beta = -0.90$ $t = -2.76$	8.86 ($p < .01$)
SGLDM → CVD	H_{7b}: Effect is stronger when IMT is higher	$\beta = 0.13$ $t = 0.53$	$\beta = 0.91$ $t = 11.91$	9.02 ($p < .01$)
GLDS → CVD	H_{7c}: Effect is stronger when IMT is higher	$\beta = 0.15$ $t = 2.19$	$\beta = -0.13$ $t = -1.17$	9.68 ($p < .01$)
SFM → CVD	H_{7d}: Effect is stronger when IMT is higher	$\beta = 0.14$ $t = 1.23$	$\beta = 0.25$ $t = 3.59$	9.09 ($p < .01$)
LTEM → CVD	H_{7e}: Effect is stronger when IMT is higher	$\beta = 0.12$ $t = 1.10$	$\beta = 0.23$ $t = 2.95$	8.60 ($p < .01$)
FDTA → CVD	H_{7f}: Effect is stronger when IMT is higher	$\beta = 0.05$ $t = 0.44$	$\beta = 0.21$ $t = 0.98$	2.44 ($p > .10$)

.01), as opposed to low IMT ($\beta = 0.12$, $t = 1.10$, $p > .10$).

Finally, the moderator was found to have no statistically significant effect ($\Delta\chi^2 = 2.44$, $p > .10$) in the case of the sixth link, FDTA → CVD (H_{7f}).

4. Discussion

The present study collectively demonstrated and verified the links between CVD and several IMC TFs, as per the proposed structural model, as presented in Table 4. Moreover, the link between IMT and CVD is also verified in the form of SEM moderation. As a result, the method proposed in this study could be used to predict future CVD events. It must be noted that no other study has been conducted in the current literature assessing the impact of IMC TFs, together with IMT, on evaluating the CVD risk, using the multifold analysis provided by SEM.

The main results of the current study, as shown in Tables 2–5, can be summarized as follows:

(i) The 6 TFs groups (SF, SGLDM, GLDS, SFM, LTEM, FDTA) tested here fit the conceptual measurement model very well (see also Fig. 2, Table 2 and Table 3). All fit indices, as well as statistics such as β, t, α, ρ, AVE are within acceptable ranges. Particularly high values arise for the TFs SGLDM (Spatial Gray Level Dependence) and SFM (Statistical Feature Matrix).

(ii) The model's 6 hypothesized paths (H_1–H_6) for the impact of each TFs group on CVD were tested (see also Table 4), with 5 of them accepted for p-values between 0.04 and 0.07; one should note here that these results point to a fairly strong link between the TFs and CVD. Still, TFs SGLDM and SFM, with $p = .04$ seem to be the TFs with the strongest link with CVD risk.

(iii) The role of the IMT as a moderator between each of the TFs proposed and CVD was also tested, yielding significant results for 5 out of 6 hypotheses (H_{7a}–H_{7e}) tested (see also Table 5), all yielding p-values < 0.01.

(iv) Furthermore, the CVD risk for the male vs. female subjects, but also how the risk is increased with increasing age were tested in the form of control effects (see also Table 4). Both controls showed a significant effect on CVD risk. In particular CVD risk increases with age (as expected), while female subjects have higher risk of CVD, according to the sample studied.

The findings of this study further verify the role that IMC TFs could play in additionally aiding CVD diagnostics and prognosis, as also previously shown [7,24,32,33,34].

Using the IMT as a moderator, instead of antecedent (latent variable) [9], enhances the precision of previously studied models [6,9], where non-complete, preliminary, with not very good fit (see also Table 1) SEM models were studied. Initially SEM was employed in order to estimate the association between IMT and IMC TFs [6]. Then, a step forward was attempted with CVD entering the picture [9]. In the current study the role of IMT as a moderator and the effect of gender and age were also tested. As previously stated in the literature, various genetic, biological and environmental variables can activate the atherosclerosis course in the form of textural changes in the CCA wall, which represent early alterations [3,7].

As already mentioned in Section 1, SEM has been employed for IMT/CVD related studies from a different perspective than the current study [18,19]. In particular, SEM was further utilized to clarify the direct and indirect pathways connecting obesity and other risk factors with CCA IMT, with IMT manually measured in CCA ultrasound images of 784 children and adolescents (10–24 years old) [35]. It was shown that blood pressure and age were the major factors with direct effect on IMT and that CVD risk was associated with increased IMT. It was also demonstrated that blood glucose had an independent direct association with IMT, which was enriched with diabetic subjects. The study was then repeated [36], demonstrating that baseline body mass index and mean blood pressure directly influences the increase of IMT. This time, baseline glucose and age showed no direct effect, whereas the period of follow-up (change in age) and change in glucose had in fact a direct effect. Changes in glucose showed the greatest direct effect. The study concluded that preventing obesity and hypertension early in adolescence, as well as preventing the shift from normoglycemia to impaired glucose tolerance, are required to decrease age-related vascular alterations. To our knowledge, there are no other studies in the literature using SEM to assess CVD risk for the L vs. R CCA based on extracted TFs.

On the other hand, there exists a number of other studies in the literature looking into the relationships between extracted IMC TFs and CVD risk. In particular, the correlations between several TFs, retrieved from the IMC of CVD patients, with CVD, were investigated [7,37], with TFs identified as possibly linked to the prevalence of the CVD. More specifically, it has been demonstrated that IMC TFs can aid in understanding the potential mechanisms associated with the early development of increased CCA IMT in CVD disease [7]. Furthermore, it is possible to utilize various TFs for the L and R CCA sides, which may correspond inversely with the IMT. Also, a study examined correlations between the L and R CCA sides in 149 patients with coronary artery disease [24]; there were no significant differences in IMT between the L vs. R CCA sides. The authors suggested that the lack of significant differences could be attributed to the small sample size and the characteristics of the population studied. Additionally, they observed that the L and R CCA IMT had varying predictive values for CVD events, indicating different associations between each side and CVD risk factors and clinical outcomes. Another study discovered a correlation between the CCA IMT and the presence of CVD, as well as lower extremity arterial atherosclerosis on both the L and R CCA sides [38]. The authors concluded that a combination of near and far wall measurements of the CCA could be a reliable indicator of CVD. In addition, a study conducted on 1655 patients about the relationship between CCA IMT and the presence of CVD risk factors [33]. The study also looked at how the degree of distal internal carotid stenosis and the proximal CCA resistive index correlated with the IMT. The results obtained showed significant differences between the L and R CCA sides, with higher IMT on the L side (L CCA: 0.97 ± 0.21 mm, $p < .001$; R CCA: 0.95 ± 0.19 mm, $p < .001$). Other independent results confirmed the relation of CVD risk factors with age as being the most relevant [10], while increased wall shear stress was noted in the L CCA side. It has also been suggested in the literature that the progression of the IMT speeds up in older individuals, potentially explaining the variation in IMT between older and younger patients [11]. It has also been hypothesized that, if mechanical shear stress plays a role in hastening the development of atherosclerosis in the L CCA side, it may take a considerable amount of time for this effect to become apparent.

Note that, to the best of our knowledge, there is still no progressive study to establish the correlation of the mentioned IMC TFs with CVD. Additional research is necessary to clarify the above points of interest. The IMT estimation changes in the mechanical properties of the CCA wall, combinations of TFs with other clinical factors, as well as the CCA sides might be important areas of interest due to their potential significance in order to indicate the existence of early CVD. The above-mentioned changes can be detected through the analysis of the CCA wall stiffness, utilizing techniques such as diameter change estimation, artery distensibility, or strain imaging [39]. There is a higher prevalence of endarterectomies on the L side [29], which may be influenced by increased shear forces in the L CCA.

There are a number of limitations in the present study. More specifically, the study is limited by the CVD dysfunction of both the L and R CCA arteries, which can be influenced by various factors [40,41]. Moreover, the combination of acoustic shadowing and intense speckle noise complicates the visual and automatic analysis of ultrasound images [20]. Images of low quality, which have poor visual clarity, were not included in this study nor were they identified by the experts [20,42]. In the segmentation experiments, images with significant

echolucency and calcification were omitted. This exclusion applies to 40 (out of 528) images from the normal (non-CVD) group and 8 (out of 84) images from the CVD group, accounting for 7.5 % and 9.5 % of the total number of images analyzed in each group, respectively. Moreover, inaccuracies in estimating and placing the initial snake contour, which was used for the automated segmentation of the IMC, can lead to segmentation errors, potentially causing the contour to be trapped in local minima or false edges [42,43]. It is crucial to position the contour as close to the area of interest as possible to avoid converging to the wrong location [5,6]. The parameters for each processing step were carefully chosen to optimize performance, including image normalization, despeckle filtering [20], moving pixel window size, number of iterations, IMC contour initialization, and snake's segmentation [4,5]. In <5 % of cases in this study, the initial snake contour positioning was found to be incorrect.

As mentioned above, future work could investigate the possibility of using additional combinations of the IMC TFs extracted, combined with clinical, as well as other genetic features in order to estimate a more accurate CVD risk. A repetition of the SEM model for other samples is of utmost importance as well.

5. Conclusions

In the current study, the moderating effect of the IMT for the links between TFs extracted from the IMC of the CCA and CVD, was investigated using SEM. It turned out that 5 out of 6 TFs tested, fit the conceptual model very well (e.g., NFI = 0.94), with 5 hypothesized paths for the impact of each TF group on CVD confirmed.

Based on the findings of the present study, it can be confidently claimed that TFs recovered from the IMC of the CCA may provide complementary information for the CVD risk. The proposed procedure, supported by SEM analysis, might be used in a future study to forecast CVD occurrences by comparing the L and R CCA sides. IMC TFs, using IMT as moderator, may thus provide additional information about the existence of clinical CVD and the risk of stroke.

The usefulness of IMC TFs in predicting future CVD events should be studied further in future studies. A similar study can also be performed utilizing other accessible IMC TFs, as well as combinations of them, in conjunction with IMT as moderator, as determined by a preliminary factor analysis.

All in all, the SEM methodology, as proposed in the present study, could eventually be at least used as a supportive tool to complement existing analyses for evaluating the CVD risk.

CRediT authorship contribution statement

George Evripides: Writing – review & editing, Writing – original draft, Software, Methodology, Investigation, Formal analysis, Conceptualization. **Christos P. Loizou:** Writing – review & editing, Writing – original draft, Supervision, Software, Methodology, Investigation, Formal analysis, Conceptualization. **Paul Christodoulides:** Writing – review & editing, Writing – original draft, Supervision, Software, Methodology, Investigation, Formal analysis, Conceptualization.

Declaration of competing interest

The authors declare that they have no known competing financial interests or personal relationships that could have appeared to influence the work reported in this paper.

Data availability

The data that has been used is confidential.

References

[1] D. Murugan, L. Rangasamy, The use of antimicrobial biomaterials as a savior from post-operative vascular graft-related infections, Results. Eng. (2022) 16.

[2] T.A. Sathi, R. Jany, R.Z. Ela, A.K.M. Azad, S.A. Alyami, M.A. Hossain, I. Hussain, An interpretable electrocardiogram-based model for predicting arrhythmia and ischemia in cardiovascular disease, Results. Eng. (2024).

[3] T. Elatrozy, A.N. Nicolaides, T. Tegos, A. Zarka, M. Griffin, M. Sabetai, The Effect of B-Mode Ultrasonic Image Standardization of the Echodensity of Symptomatic and Asymptomatic Carotid Bifurcation Plaque, Int. Angiol 17 (1998) 179–186.

[4] C.P. Loizou, A.N. Nicolaides, N. Georghiou, M. Griffin, E. Kyriakou, C.S. Pattichis, A Comparison of Ultrasound Intima-Media Thickness Measurements of the Left and Right Common Carotid Artery, IEEE J. Transl. Eng. Health Medic 3 (2015) 1–10.

[5] C.P. Loizou, C.S. Pattichis, A.N. Nicolaides, M. Pantzaris, Manual and automated media and intima thickness measurements of the common carotid artery, in: 56, 2009, pp. 983–994.

[6] C.P. Loizou, G. Evripides, P. Christodoulides, Structural Equation Modelling for Stroke Risk Assessment of the Common Carotid Artery Based on Texture Analysis, in: IEEE 6th Eur. Conf. Electr. Engin. & Comput. Science (ELECS), Bern, Switzerland, 2022, pp. 31–35.

[7] C.P. Loizou, E. Kyriakou, M.B. Griffin, A.N. Nicolaides, C.S. Pattichis, Association of Intima-Media Texture with Prevalence of Clinical Cardiovascular Disease, IEEE Trans. Ultra-sonics, Ferroelectrics Freq. Control 68 (2021) 3017–3026.

[8] A. Sonaglioni, E. Piergallini, A. Naselli, G.L. Nicolosi, A. Ferrulli, S. Bianchi, M. Lombardo, G. Ambrosio, The Effect of Gestational Diabetes Mellitus on Carotid Artery Intima-Media Thickness in and after Pregnancy: a Systematic Review and Meta-Analysis, Acta Diabetol. 61 (2024) 139–149.

[9] G. Evripides, Christodoulides, C.P Loizou, Texture Analysis Contribution to Evaluate the Common Carotid Artery's Cardiovascular Disease (CVD) Risk Using Structural Equation Modeling, in: 20th International Conference, CAIP 2023, Limassol, Cyprus, 2023.

[10] L. Lind, J. Andersson, A. Larsson, B. Sandhagen, Shear Stress in the Common Carotid Artery Is Related to Both Intima-Media Thickness and Echogenecity: the Prospective Investigation of the Vasculature in Uppsala Seniors Study, Clin. Hemorheol. Microcirculat 43 (2009) 299–308.

[11] P.L. Allan, P.I. Mowbray, A.J. Lee, F.G.R. Fowkes, Relationship between Carotid Intima-Media Thickness and Symptomatic and Asymptomatic Peripheral Arterial Disease. The Edinburgh Artery Study, Stroke 28 (1997) 348–353.

[12] P. Tarka, An Overview of Structural Equation Modeling: its Beginnings, Historical Development, Usefulness and Controversies in the Social Sciences, Qual. Quant. 52 (2018) 313–354.

[13] R.G. Hancock, Fortune Cookies, Measurement Error and Experimental Design, Hancock, R.G 2 (2003) 3. –3.

[14] L.C. Leonidou, B. Aykol, T.A. Fotiadis, A. Zeriti, P. Christodoulides, The Role of Exporters' Emotional Intelligence in Building Foreign Customer Relationships, J. Int. Market. 27 (2019) 58–80.

[15] L.C. Leonidou, B. Aykol, S. Spyropoulou, P. Christodoulides, The power roots and Drivers of infidelity in international business relationships, Ind. Market. Manage. 78 (2019) 198–212.

[16] R. Bagozzi, Y. Yi, On the evaluation of structural equation models, J. Acad. Mark. Sci. 16 (1988) 74–94.

[17] J.C. Anderson, D.W. Gerbing, Structural equation modeling in practice: a review and recommended two-step approach, Psychol. Bull. 103 (1988) 411–423.

[18] J.H. Fergenbaum, S. Bruce, J.D. Spence, W. Lou, A.J. Hanley, C. Greenwood, T. K. Young, Carotid atherosclerosis and a reduced likelihood for lowered cognitive performance in a canadian first nations population, Euroepidemiology 33 (2009) 321–328.

[19] Z. Gao, L.M. Dolan, E.M. Urbina, Structural Equation Modeling Demonstrates Only an Indirect Effect of Obesity on Carotid Intima-Media Thickness in Adolescents and Young Adults, Circulation 130 (2014) 13223. –13223.

[20] C.P. Loizou, C.S. Pattichis, C.I. Christodoulou, R.S.H. Istepanian, M. Pantzaris, A. N. Nicolaides, Comparative Evaluation of Despeckle Filtering in Ultrasound Imaging of the Carotid Artery, IEEE Trans. Ultras. Ferroel. Freq. Contr 52 (2005) 1653–1669.

[21] L.C. Leonidou, B. Aykol, J. Larimo, L. Kyrgidou, P. Christodoulides, Enhancing international buyer-seller relationship quality and long-term orientation using emotional intelligence: the moderating role of foreign culture, Manage. Int. Rev. 61 (2021) 365–402.

[22] R.M. Haralick, K. Shanmugam, I. Dinstein, Texture Features for Image Classification, IEEE Trans. Syst. Man. Cyber. SMC 3 (1973) 610–621.

[23] J.S. Weszka, C.R. Dyer, A. Rosenfield, A Comparative Study of Texture Measures for Terrain Classification, IEEE Trans. Syst. Man. Cyber. SMC 6 (1976) 269–285.

[24] S.W.L. Lee, et al. Side Differences of Carotid Intima-Media Thickness in Predicting Cardiovascular Events among Patients with Coronary Artery Disease, Angiology 62 (2011) 231–236.

[25] M. Amadasun, R. King, Textural Features Corresponding to Textural Properties, IEEE Trans. Syst. Man. & Cyber 19 (1989) 1264–1274.

[26] C.-M. Wu, Y.-C. Chen, K.-S. Hsieh, Texture Features for Classification of Ultrasonic Liver Images, IEEE Trans. Med. Imag 11 (1992) 141–152.

[27] R.R. Bagozzi, Y. Yi, On the Evaluation of Structural Equation Models, J Acad Mark Sci 16 (1988) 74–94.

[28] J.F. Hair, W.C. Black, B.J. Babin, R.E. Anderson, Multivariate Data Analysis, Cengage Learn. EMEA (2018).

[29] C. Fornell, D.F. Larcker, Evaluating structural equation models with unobservable variables and measurement error, J. Market. Res. 28 (1981) 39–50.

[30] J.C. Nunnally, I.H Berstein, Psychometric Theory, 3rd ed., McCraw-Hill. Inc, New York, 1994.
[31] P.M. Podsakoff, D.W. Organ, Self-Reports in Organizational Research: problems and Prospects, J. Manage 12 (1986) 531–544.
[32] N. Venkatraman, J.E. Prescott, Environment-strategy coalignment: an empirical test of its performance implications, Strateg. Manage J. 11 (1990) 1–23.
[33] M.L. Bots, P.T.V.M. De Jong, A. Hofman, D.E.Left Grobbee, Right, near or far wall common carotid Intima-media thickness measurements: associations with cardiovascular disease and lower extremity arterial atherosclerosis, J. Clin. Epidemiol 50 (1997) 801–807.
[34] B.G. Maxwell, J.G. Maxwell, C.C. Brinker, Left-side preference in carotid endarterectomies, Amer. Surgeon 66 (2000) 793–796.
[35] Z. Gao, P.R. Khoury, C.E. McCoy, A.S. Shah, et al., Adiposity has no direct effect on carotid intima-media thickness in adolescents and young adults: use of structural equation modeling to elucidate indirect & direct pathways, Atheroscler 246 (2016) 29–35.
[36] Z. Gao, P.R. Khoury, L.M. Dolan, E.M. Urbina, Direct and indirect effects of obesity on progression of carotid arterial injury in youth, Pediatr. Obes. 29 (2021) 1892–1898.
[37] C.C. Mitchell, C.E. Korcarz, A.D. Gepner, R. Nye, et al., Carotid artery echolucency, tex-ture features, and incident cardiovascular disease events the MESA study, J Am Heart As-soc 8 (2019) 1–16.
[38] B.G. Maxwell, J.G. Maxwell, C.C. Brinker, Left-side preference in carotid endarterectomies, Amer. Surgeon 66 (2000) 793–796.
[39] M. Cinthio, A.R. Ahlgren, T. Jansson, A. Eriksson, H.W. Persson, K. Lindstrom, Evaluation of an ultrasonic echo-tracking method for measurements of arterial wall movements in two dimensions, IEEE Trans. Ultrason., Ferroelectr., Freq. Control 52 (2005) 1300–1311.
[40] Y. Arbel, N. Maharshak, A. Gal-Oz, I. Shapira, S. Berliner, N.M. Bornstein, IEEE Trans. Ultrason., Ferroelectr., Freq. Control. *Acta Neurol. Scandinavica* 115 (2007) 409–412.
[41] X. Luo, Y. Yang, T. Cao, Z. Li, Differences in Left and Right Carotid Intima-Media Thickness and the Associated Risk Factors, Clin. Radiol 66 (2011) 393–398.
[42] C.P. Loizou, A Review of Ultrasound Common Carotid Artery Image and Video Segmentation Techniques, Med. Biol. Eng. Comput 52 (2014) 1073–1093.
[43] S. Delsanto, F. Molinari, P. Giustetto, W. Liboni, S. Badalamenti, J.S. Suri, Characterization of a Completely User-Independent Algorithm for Carotid Artery Segmentation in 2-D Ultrasound Images, IEEE Trans. Instrum. Meas 56 (2007) 1265–1274.